*Proceedings of the 10th World Congress on Electrical Engineering and Computer Systems and Sciences (EECSS'24)*
*Barcelona, Spain - August 19 - 21, 2024*
*Paper No. CIST 173*
*DOI: 10.11159/cist24.173*

# Impact Force Identification in Cobots: a Preliminary Work

**Fabio Zanoletti[1], Cinzia Amici[2], Alberto Borboni[3]**
[1,2,3] University of Brescia, Department of Industrial and Mechanical Engineering,
Via Branze 38, 25123, Brescia, Italy
[1]fabio.zanoletti@unibs.it
[2]cinzia.amici@unibs.it
[3]alberto.borboni@unibs.it

***Abstract*** – Nowadays, cobots have become common in manufacturing industry collaborating with human agents and are predicted to be increasingly part of our lives. Whether it is industrial or service robots, the recent trend is to focus on what has been called human-robot collaboration (HRC). This poses a critical issue regarding the safety of human agents interacting with robot agents. Detecting a collision and executing an appropriate control strategy to reduce impact damages has been proven to be as an effective way to ensure a safe environment for human agents. This paper evaluates an approach for the complete identification of impact action in terms of point of application, intensity, and direction under some illustrative assumptions on robot geometry and system dynamics using only the sensors already present in the robot control system. Simulations have been carried out and their results suggest that the presented approach might be viable for collision detection, isolation, and identification.

***Keywords*:** Robotics, Robots, Cobots, Collision Detection, Collision Isolation, Collision Identification.

## 1. Introduction

Robots directly interacting with humans are spreading in various application areas, such as cobots in industry [1,2], as medical robots or as other types of service robots [3–5], sharing spaces or work functions. In all these areas, the robot must be able to evaluate external actions in kinematic and dynamic terms, incrementing its computational abilities [6]. In particular, this paper wants to focus on applications in industry (cobots) and the safety aspects associated with undesired mechanical actions exchanged between human and robot in terms of collisions.

The main safety systems in robotic environments are reported in [7] and can be classified into two macro-categories: collision avoidance and minimizing injury caused by the collision. The first approach intends to prevent collisions using collision avoidance systems, but this requires some knowledge of the environment and the use of advanced motion planning techniques. Given these reasons and the fact that in collaborative tasks direct contact may be desired, many robotic systems consider that impacts may be inevitable, and they work to ensure the least amount of damage. This can be achieved with mechanical compliance systems or with safety strategies involving contact detection. The latter consists of actively detecting and isolating the impact to actuate different robot control strategies to ensure the operator's safety. Examples of the different control strategies are discussed in [8].

Collision detection and isolation are a crucial part and can be implemented by using sensitive skins that envelope the robot structure [9] or by using the proprioceptive sensors of the robot. Different methods to detect and estimate the contact forces on a robot by only using the already available sensors inside it have been documented in [10]. The method in [11] is based on the premise that the collision can be detected as a faulty behavior in the robot's actuators and its effects can be observed by comparing the applied torque with the nominal control torque. In [12] a method based on the generalized momentum of the robot is presented and in [8] and [13] it has been validated for two different commercially available 7-dof manipulators. Once the collision is detected the impact point can be estimated via pseudoinversion [13], via the Contact Particle Filter (CPF) described in [14] or with both [15].

This paper focuses on the complete identification of impact action in terms of point of application, intensity, and direction using only the sensors already present in the robot control system in the case of a three degrees of freedom planar manipulator.

## 2. Materials and methods

### 2.1. Materials

The proposed collision detection, isolation, and identification approach is tested on a simulation of a *3 degrees of freedom planar robot* (Fig. 1) which consists of three links and three joints, allowing it to move in the vertical plane *Oxz*. Its kinematic chain is described according to the Denavit-Hartenberg parameters in Table 1. Each reference frame $O_iX_iY_iZ_i$ associated with the joint coordinate $q_i$ is located with the origin in the $i^{th}$ joint and solid with the $i^{th}$ link.

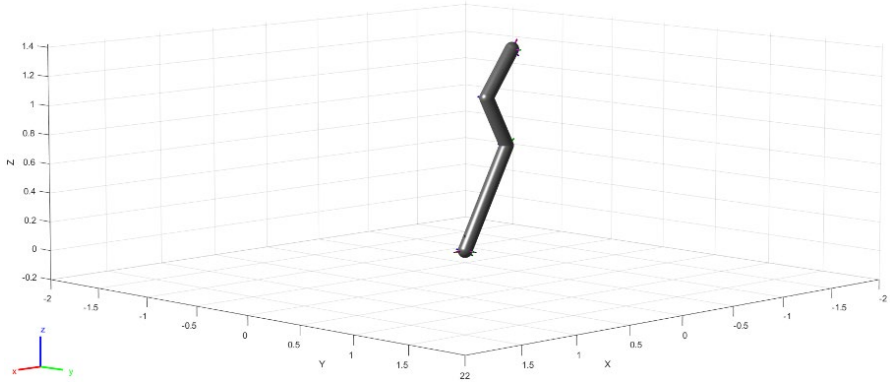


Fig. 1. Matlab simulation of the 3DoF Planar Robot.

The robot is modelled in Matlab using the *rigidBodyTree* class. In this case, the manipulator is considered as a system composed of *n=3* rigid bodies with three rotational joints. The simulated robot is constituted by *rigidBody* objects representing the links, each with its associated inertia and geometrical attributes, connected by *rigidBodyJoint* objects that simulate the robot's motors.

Table 1. D-H parameters of the 3-dof planar robot. The parameters considered are length *a*, torsion α, offset *d*, and rotation *Θ*.

| a [mm] | α [rad] | d [mm] | Θ [rad] |
|---|---|---|---|
| 0 | -π/2 | 0 | $q_1$ |
| L1 | 0 | 0 | $q_2$ |
| L2 | 0 | 0 | $q_3$ |
| L3 | π/2 | 0 | - |

### 2.2. Methods: Theoretical Background

The dynamics for an open-chain serial manipulator with *n* motorized joints can be described, as in Eq. (1), where $\boldsymbol{Q}, \dot{\boldsymbol{Q}}, \ddot{\boldsymbol{Q}} \in \mathbb{R}^n$ are the generalized joint positions, velocities, and accelerations respectively, $\boldsymbol{\mathcal{M}}(\boldsymbol{Q}) \in \mathbb{R}^{n\times n}$ is the symmetric, positive definite, inertia matrix of the robot, $\boldsymbol{\mathcal{V}}(\boldsymbol{Q}, \dot{\boldsymbol{Q}})\dot{\boldsymbol{Q}} \in \mathbb{R}^n$ is the Coriolis and Centrifugal forces vector, and $\boldsymbol{G}(\boldsymbol{Q}) \in \mathbb{R}^n$ is the gravitational and friction forces vector. The motor torques are represented by $\boldsymbol{\tau}_m \in \mathbb{R}^n$.

$$\boldsymbol{\mathcal{M}}(\boldsymbol{Q})\ddot{\boldsymbol{Q}} + \boldsymbol{\mathcal{V}}(\boldsymbol{Q}, \dot{\boldsymbol{Q}})\dot{\boldsymbol{Q}} + \boldsymbol{G}(\boldsymbol{Q}) = \boldsymbol{\tau}_m + \boldsymbol{\tau}_{ext} \tag{1}$$

The external joint torques are contained in $\boldsymbol{\tau}_{ext} \in \mathbb{R}^n$ and are correlated to the external forces and moments wrench $\boldsymbol{F}_{ext} = \left[F_x, F_y, F_z, T_x, T_y, T_z\right]^T$ by the relation in Eq. (2), where $\boldsymbol{J}_c(\boldsymbol{Q}) \in \mathbb{R}^{6\times n}$ is the geometric Jacobian associated to the impact point. The Jacobian $\boldsymbol{J}_c(\boldsymbol{Q})$, by its definition, correlates the linear and angular velocity of the collision frame located in the impact point $\boldsymbol{P}_c$ to the joint velocity $\dot{\boldsymbol{Q}}$.

$$\boldsymbol{\tau}_{ext} = \boldsymbol{J}_c^T(\boldsymbol{Q})\boldsymbol{F}_{ext} \tag{2}$$

By considering Eq. (1), is possible to estimate the external joint torque as its expression is in Eq. (3).

$$\tilde{\boldsymbol{\tau}}_{ext} = \boldsymbol{\mathcal{M}}(\boldsymbol{Q})\ddot{\boldsymbol{Q}} + \boldsymbol{\mathcal{V}}(\boldsymbol{Q}, \dot{\boldsymbol{Q}})\dot{\boldsymbol{Q}} + \boldsymbol{G}(\boldsymbol{Q}) - \boldsymbol{\tau}_m \tag{3}$$

A collision can be detected whenever the external joint torques are non-zero $\tilde{\boldsymbol{\tau}}_{ext} \neq \vec{0}$. In this case, the external torque estimation requires the knowledge of the dynamic model, and the direct measurement of $\boldsymbol{Q}, \dot{\boldsymbol{Q}}, \ddot{\boldsymbol{Q}}$ and of the motor torques $\boldsymbol{\tau}_m$. If a robot is not equipped with torque sensors, the motor torques $\boldsymbol{\tau}_m$ can be estimated by the relation $\boldsymbol{\tau}_m = \boldsymbol{K}_i \boldsymbol{i}_m$ which correlates the motor currents $\boldsymbol{i}_m$ to the torques by the torque constants in the diagonal matrix $\boldsymbol{K}_i$.

The collision can be isolated by determining the collided link and the contact point. The impacted link can be found by observing the external joint torques. The torque vector assumes the form $\tilde{\boldsymbol{\tau}}_{ext} = \left[\tau_{ext,1}, \dots, \tau_{ext,j_c}, 0, \dots, 0\right]^T$, so the impacted link is *link* $j_c$. The contact point $\boldsymbol{P}_c$ is represented by the cartesian coordinates $[x_c, y_c, z_c]$ and, in general, its isolation can be obtained only for certain types of collisions [10]. Given that $\boldsymbol{J}_c(\boldsymbol{Q}) \in \mathbb{R}^{6\times n}$, the contact point isolation is possible only if the impacted link index $j_c \geq 6$ and no contact moments are present, so the contact wrench must be in the form $\boldsymbol{F}_{ext} = \left[F_x, F_y, F_z, 0,0,0\right]^T$ where $F_x$, $F_y$, and $F_z$ are the cartesian components of the impact force.

Once the contact point is established, the planar contact forces can be estimated by the general relation in Eq. (4), where $\left(\boldsymbol{J_c}(\boldsymbol{Q})^{\boldsymbol{T}}\right)^+$ is the pseudoinverse of the transposed collision Jacobian. The collision identification is impossible for impacts happening on links close to the base and in the case of the proximity to singular configurations [10]. In these cases, the contact Jacobian lacks full rank.

$$\widetilde{\boldsymbol{F}}_{ext} = \left(\boldsymbol{J_c}(\boldsymbol{Q})^{\boldsymbol{T}}\right)^+ \tilde{\boldsymbol{\tau}}_{ext} \tag{4}$$

Even though the described method neglects joint compliances, the same approach may be feasible as an extended dynamic model can be adopted, as in Eq. (5), where the new generalized coordinates are $\boldsymbol{Q} \in \mathbb{R}^n$, that represents the link position, and $\boldsymbol{\theta} \in \mathbb{R}^n$, that represents the motor position. The matrices $\boldsymbol{K} = diag(K_{e,i}) \in \mathbb{R}^{n\times n}$ and $\boldsymbol{D} = diag(D_i) \in \mathbb{R}^{n\times n}$ are respectively the joint stiffness matrix and the joint damping matrix whereas $\boldsymbol{\tau}_J$ is the elastic torque transmitted through the joints.

$$\begin{cases} \boldsymbol{\mathcal{M}}(\boldsymbol{Q})\ddot{\boldsymbol{Q}} + \boldsymbol{\mathcal{V}}(\boldsymbol{Q}, \dot{\boldsymbol{Q}})\dot{\boldsymbol{Q}} + \boldsymbol{G}(\boldsymbol{Q}) + \boldsymbol{K}(\boldsymbol{Q} - \boldsymbol{\theta}) = \boldsymbol{D}(\dot{\boldsymbol{Q}} - \dot{\boldsymbol{\theta}}) \\ \boldsymbol{\tau}_J = \boldsymbol{K}(\boldsymbol{Q} - \boldsymbol{\theta}) \end{cases} \tag{5}$$

The tested collision detection, isolation and identification method requires the definition of the dynamic model of the robot. At this stage, additional simplifications are adopted: the links are considered as ideal rods; the end effector is considered as a point mass; the 3D geometry of the links is neglected so the collision occurs along the axis of the link; the joints are considered ideal without friction and elasticities. Thus, the robot model is defined as presented in (Fig. 2).

For planar and Shöenflies systems, the matrices and vectors in Eq. (3), can be determined with the approach described in [16], i.e., by adopting as extended coordinates: the set of coordinates of the centers of mass, the set of coordinates of all application points of external/inertial forces and torques, and the angular position of the links. For the 3-dof planar robot with joint coordinates $\boldsymbol{Q} = [q_1, q_2, q_3]$ and with the three links *link*$_1$, *link*$_2$, and *link*$_3$, an analytical formulation for $\boldsymbol{\mathcal{M}}(\boldsymbol{Q})$, $\boldsymbol{\mathcal{V}}(\boldsymbol{Q}, \dot{\boldsymbol{Q}})\dot{\boldsymbol{Q}}$, and $\boldsymbol{G}(\boldsymbol{Q})$ has been written in Eq. (6), Eq. (7), and Eq. (8) respectively.

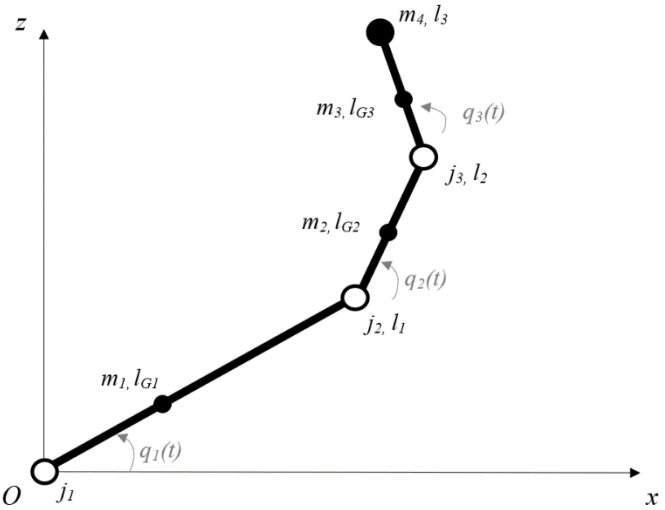


Fig. 2. Model of the 3-dof planar robot with ideal bodies and joints.

Each link is considered as an ideal rod with length $l_j$, mass $m_j$, moment of inertia $I_{Gj}$ and the center of mass is located at a distance $l_{Gj}$ from the upstream joint. The end effector is considered as a point mass $m_4$ located at the end of the last link.

$$\boldsymbol{\mathcal{M}}(\boldsymbol{Q}) = \begin{bmatrix} \mathcal{M}_{11} & \mathcal{M}_{12} & \mathcal{M}_{13} \\ \mathcal{M}_{21} & \mathcal{M}_{22} & \mathcal{M}_{23} \\ \mathcal{M}_{21} & \mathcal{M}_{22} & \mathcal{M}_{33} \end{bmatrix} \tag{6}$$

$$\begin{aligned}
\mathcal{M}_{11} &= I_1 + m_1 l_{G1}^2 + I_{G2} + m_2 l_{G2}^2 + I_{G3} + m_3 l_{G3}^2 + I_{G4} + m_4 l_3^2 + (m_2 + m_3 + m_4) l_1^2 + (m_3 + m_4) l_2^2 \ldots \\
&\quad + 2(m_2 l_{G2} + m_3 l_2 + m_4 l_2) l_1 \cos q_2 + 2(m_3 l_{G3} + m_4 l_3)(l_1 \cos(q_2 + q_3) + l_2 \cos q_3) \\
\mathcal{M}_{22} &= I_{G2} + m_2 l_{G2}^2 + I_{G3} + m_3 l_{G3}^2 + I_{G4} + m_4 l_3^2 + (m_3 + m_4) l_2^2 + 2(m_3 l_{G3} + m_4 l_3) l_2 \cos q_3 \\
\mathcal{M}_{33} &= I_{G3} + m_3 l_{G3}^2 + I_{G4} + m_4 l_3^2 \\
\mathcal{M}_{12} &= \mathcal{M}_{21} = I_{G2} + m_2 l_{G2}^2 + I_{G3} + m_3 l_{G3}^2 + I_{G4} + m_4 l_3^2 + (m_3 + m_4) l_2^2 \ldots \\
&\quad + (m_2 l_{G2} + m_3 l_2 + m_4 l_2) l_1 \cos q_2 + 2(m_3 l_{G3} + m_4 l_3) l_2 \cos q_3 + (m_3 l_{G3} + m_4 l_3) l_1 \cos(q_2 + q_3) \\
\mathcal{M}_{13} &= \mathcal{M}_{31} = I_{G3} + m_3 l_{G3}^2 + I_{G4} + m_4 l_3^2 + (m_3 l_{G3} + m_4 l_3)(l_2 \cos q_3 + l_1 \cos(q_2 + q_3)) \\
\mathcal{M}_{23} &= \mathcal{M}_{32} = I_{G3} + m_3 l_{G3}^2 + I_{G4} + m_4 l_3^2 + (m_3 l_{G3} + m_4 l_3) l_2 \cos q_3
\end{aligned}$$

$$\boldsymbol{\mathcal{V}}(\boldsymbol{Q}, \dot{\boldsymbol{Q}})\dot{\boldsymbol{Q}} = \begin{bmatrix} \mathcal{V}_1 \\ \mathcal{V}_2 \\ \mathcal{V}_3 \end{bmatrix} \tag{7}$$

$$\begin{aligned}
\mathcal{V}_1 &= -\big((m_2 l_{G2} + m_3 l_2 + m_4 l_2) \sin q_2 + (m_3 l_{G3} + m_4 l_3) \sin(q_2 + q_3)\big) l_1 \dot{q}_2^2 \ldots \\
&\quad -\big((m_3 l_{G3} + m_4 l_3)(l_2 \sin q_3 + l_1 \sin(q_2 + q_3))\big) \dot{q}_3^2 \ldots \\
&\quad -2\big((m_2 l_{G2} + m_3 l_2 + m_4 l_2) \sin q_2 + (m_3 l_{G3} + m_4 l_3) \sin(q_2 + q_3)\big) l_1 \dot{q}_1 \dot{q}_2 \ldots \\
&\quad -2\big((m_3 l_{G3} + m_4 l_3)(l_2 \sin q_3 + l_1 \sin(q_2 + q_3))\big)(\dot{q}_1 \dot{q}_3 + \dot{q}_2 \dot{q}_3) \\
\mathcal{V}_2 &= \big((m_3 l_{G3} + m_4 l_3) \sin(q_2 + q_3) + (m_2 l_{G2} + m_3 l_2 + m_4 l_2) \sin q_2\big) l_1 \dot{q}_1^2 \ldots \\
&\quad -(m_3 l_{G3} + m_4 l_3) l_2 \sin q_3 \, (\dot{q}_3^2 + 2\dot{q}_1 \dot{q}_3 + 2\dot{q}_2 \dot{q}_3) \\
\mathcal{V}_3 &= (m_3 l_{G3} + m_4 l_3) \left((l_2 \sin q_3 + l_1 \sin(q_2 + q_3)) \dot{q}_1^2 + l_2 \sin q_3 \, \dot{q}_2^2 + 2 l_2 \sin q_3 \, \dot{q}_1 \dot{q}_2\right)
\end{aligned}$$

$$\boldsymbol{G}(\boldsymbol{Q}) = \begin{bmatrix} G_1 \\ G_2 \\ G_3 \end{bmatrix} \tag{8}$$

$$\begin{aligned} G_1 = g[&m_1 l_{G1} \cos q_1 + m_2(l_1 \cos q_1 + l_{G2} \cos(q_1 + q_2)) \dots \\ &+ m_3(l_1 \cos q_1 + l_2 \cos(q_1 + q_2) + l_{G3} \cos(q_1 + q_2 + q_3)) \dots \\ &+ m_4(l_1 \cos q_1 + l_2 \cos(q_1 + q_2) + l_3 \cos(q_1 + q_2 + q_3))] - \tau_1 \\ G_2 = g[&m_2 l_{G2} \cos(q_1 + q_2) + m_3(l_2 \cos(q_1 + q_2) + l_{G3} \cos(q_1 + q_2 + q_3)) \dots \\ &+ m_4(l_2 \cos(q_1 + q_2) + l_3 \cos(q_1 + q_2 + q_3))] - \tau_2 \\ G_3 = g[&m_3 l_{G3} \cos(q_1 + q_2 + q_3) + m_4 l_3 \cos(q_1 + q_2 + q_3)] - \tau_3 \end{aligned}$$

If the collision force wrench assumes the form $\boldsymbol{F}_{ext} = [F_x, 0, F_z]^T$, which is justified since the force is planar and the contact momentum is negligible in the case of impulsive collisions, the collision can be detected when the estimated external joint torques $\tilde{\boldsymbol{\tau}}_{ext} = \left[\tilde{\tau}_{1,ext}, \tilde{\tau}_{2,ext}, \tilde{\tau}_{3,ext}\right]^T \neq [0,0,0]^T$.

The impacted link can be isolated by examining the last non-zero term of $\tilde{\boldsymbol{\tau}}_{ext}$. For example, if $\tilde{\boldsymbol{\tau}}_{ext} = \left[\tilde{\tau}_{1,ext}, \tilde{\tau}_{2,ext}, \tilde{\tau}_{3,ext}\right]^T$ the collision happened on the third link. The collision point, which coordinates are $\boldsymbol{P}_c = [x_c, 0, z_c]^T$, can be described as the point at a distance $d_c$ along the link axis from the upstream joint $j_c$, and its Jacobian assumes the form $\boldsymbol{J}_c(\boldsymbol{Q}) \in \mathbb{R}^{3\times3}$. By considering Eq. (4) is possible to define a 3x3 system of equations to calculate the unknown variables $[F_x, F_z, d_c]$ ensuring complete isolation and identification. If a collision occurs on the first or second link the system of equations is underdetermined and additional information about the contact point or direction of application of the impact force is needed. In the case of a collision on the third link, the system can be solved and is reported in Eq. (9). In Eq. (9) $q_{12} = q_1 + q_2$, and $q_{123} = q_1 + q_2 + q_3$.

$$\begin{cases} \tilde{\tau}_{1,ext} = (l_1 \cos q_1 + l_2 \cos q_{12} + d_c \cos q_{123})F_z - (l_1 \sin q_1 + l_2 \sin q_{12} + d_c \sin q_{123})F_x \\ \tilde{\tau}_{2,ext} = (l_2 \cos q_{12} + d_c \cos q_{123})F_z - (l_2 \sin q_{12} + d_c \sin q_{123})F_x \\ \tilde{\tau}_{3,ext} = (d_c \cos q_{123})F_z - (d_c \sin q_{123})F_x \end{cases} \tag{9}$$

### 2.3. Methods: Simulations

The simulations have been carried out in Matlab environment to analyze the collision event for the robot. The manipulator is modelled using the *rigidBodyTree* class, the links are rigid bodies with cylindrical shape, the joints are ideal joints, and they move with a trapezoidal acceleration law of motion. The *rigidBody* and *rigidBodyJoint* objects parameters are reported in Table 2.

Table 2. *rigidBodyTree model* parameters for the 3-dof planar robot.

| Link | Joint Type | Length [m] | Mass [kg] | $L_G$ [m] | Radius [m] |
|---|---|---|---|---|---|
| Link1 | R | 0.8 | 10 | 0.4 | 0.05 |
| Link2 | R | 0.4 | 5 | 0.2 | 0.05 |
| Link3 | R | 0.4 | 5 | 0.2 | 0.05 |
| EE | - | - | 3 | 0 | - |

When a collision occurs, an external force is applied in the contact point (Fig. 3). The estimated external joint torques are evaluated as described by Eq. (3) given that: the joint positions, velocities, and accelerations are directly measured; the motor torques are calculated with the *inverseDynamics* function provided for the r*igidBodyTree* class; the dynamic model of the robot is defined as in Eq, (6), (7), (8). The dynamic model parameters are set to reflect potential inaccuracies in parameter estimation, i.e., in the case of links length and mass, the model parameters are ±0.002m and ±0.01kg the values in Table 2.

The collision detection, isolation and identification are executed as described and the force intensity, point and line of application are calculated. Multiple tests have been executed to consider different collision configurations, points of application, and impact forces.

Simulations of the impacts on the first and second link have been executed but additional information about the impact point and line of application of the impact force are needed to ensure a complete isolation and identification.

## 3. Results

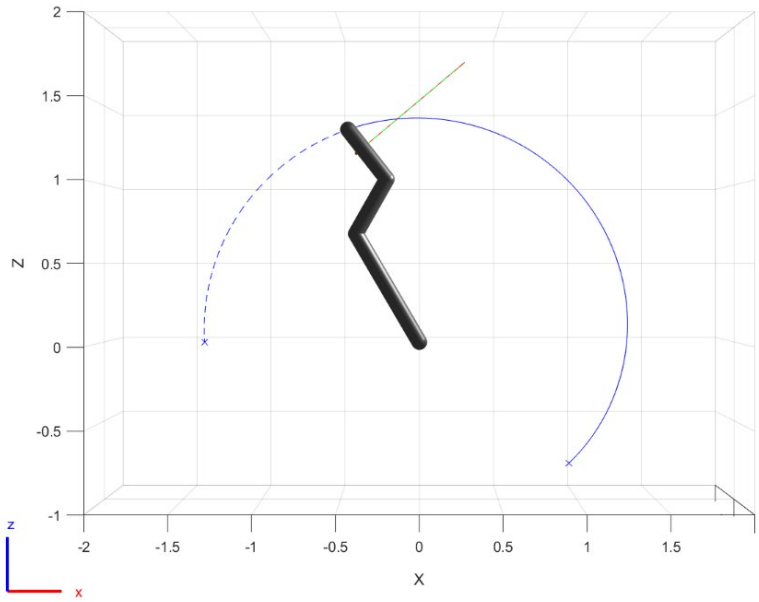


Fig. 3. Collision event for the planar robot.

The manipulator depicted in grey moves in the *Oxz* vertical plane. The desired end effector trajectory is represented by the dashed blue line, while the actual end effector trajectory is shown with the continuous blue line. The impact force is indicated by the continuous red line and the estimated impact force is indicated by the dashed green line.

With the proposed method is possible to estimate the impact force intensity, direction and point of application for collisions happening on the third link of the studied manipulator.

The estimated results are comparable to the simulated ones: the external joint torque $\tilde{\boldsymbol{\tau}}_{ext}$ is overestimated by 0.137±0.22Nm(P=95%); the force intensity $F$ is overestimated by 0.07±1.08N(P=95%); the angle of application $\alpha$ is overestimated by 0.24±1°(P=95%); the point of application $d_c$ is overestimated by 0.042±0.19m(P=95%).

## 4. Discussion

The simulations results suggest that collision detection, isolation, and identification might be feasible for the robot. Under the presented assumptions, the impacted link and the impact point can be determined, and the impact force can be estimated as in Eq. (4) and Eq. (9).

The presented method is compared with the other methods in the literature in Table 3. One potential limitation of the direct external torques estimation (Eq. (3)) is the need to measure $\boldsymbol{Q}, \dot{\boldsymbol{Q}}, \ddot{\boldsymbol{Q}}$. The measurement of the joint acceleration $\ddot{\boldsymbol{Q}}$ can pose a problem in practical applications if the robot is only capable of measuring $\boldsymbol{Q}$, as the double differentiation leads to noise. However, for robots with sensors to measure both velocity and acceleration, this might not be an issue.

For collisions occurring on the first and second link or if the robot is near a kinematic singularity, additional information is needed; otherwise, detection, isolation and identification are not possible. In these cases, the pseudo-inversion of the collision Jacobian experiences numerical problems. For collisions occurring on the last link, the method does not require additional sensors or measurements to ensure complete isolation, as three equations are sufficient in the plane.

Table 3. Comparison with the literature

| | This paper | [8] De Luca 2006 | [17] Buondonno 2016 | [13] Iskandar 2021 | [15] Zurlo 2023 |
|---|---|---|---|---|---|
| Detection | x | x | x | Multi-contact | x |
| Isolation | x | x | x | x | x |
| Identification | x | x | x | x | x |
| Method | Direct estimation. + Isolation by pseudoinversion. | Generalized momentum observer. + Isolation by pseudoinversion. | Generalized momentum observer. + Additional sensor in the base. | Generalized momentum observer. + Sensing redundancy. | Generalized momentum observer. + Energy based. + Isolation by CPF. |
| Needed measurements | $\boldsymbol{\tau_m, Q, \dot{Q}, \ddot{Q}}$ | $\boldsymbol{\tau_m, Q, \dot{Q}}$ | $\boldsymbol{\tau_m, Q, \dot{Q}, F_{base}, T_{base}}$ | $\boldsymbol{\tau_m, Q, \dot{Q}}$ | $\boldsymbol{\tau_m, Q, \dot{Q}}$ |

In a more general case, another approach might be necessary to estimate the dynamic model since the one presented in [16] is applicable only for planar and Shöenflies systems. The study of the Lagrangian of the system might be a feasible one.

An experimental evaluation is required for this approach. Subsequently, it is essential to conduct comparable tests using a broader scenario that considers three-dimensional movements and the robot's geometry.

## 5. Conclusion

A preliminary approach for the complete identification of collision forces in terms of point of application, intensity, and direction, by only using the sensors already present in the robot control system has been evaluated for an open kinematic chain. Given the specific assumptions on the robot's geometry and system dynamics, the simulated results suggest that this approach might be viable in collision detection, isolation, and identification, especially as a low-cost alternative for simple manipulators.

## References


[1] A. Borboni, R. Pagani, S. Sandrini, G. Carbone, and N. Pellegrini, "Role of Reference Frames for a Safe Human-Robot Interaction", *Sensors*, vol. 23, no. 12, 2023.

[2] C. Taesi, F. Aggogeri and N. Pellegrini, "COBOT Applications—Recent Advances and Challenges". *Robotics,* vol. 12, 2023.

[3] C. Amici, A. Borboni and R. Faglia, "A compliant PKM mesomanipulator: Kinematic and dynamic analyses", *Advances in Mechanical Engineering*, vol. 2010, no. 2, 2010.

[4] C. Amici, A. Borboni, R. Faglia, D. Fausti and P.L. Magnani, "A parallel compliant meso-manipulator for finger rehabilitation treatments: Kinematic and dynamic analysis", *IEEE/RSJ International Conference on Intelligent Robots and Systems,* IROS, art. no. 4651029, pp. 735-740, 2008.

[5] A. Borboni, J.H. Villafañe, C. Mullè, K. Valdes, R. Faglia, G. Taveggia and S. Negrini, "Robot-Assisted Rehabilitation of Hand Paralysis After Stroke Reduces Wrist Edema and Pain: A Prospective Clinical Trial", *Journal of Manipulative and Physiological Therapeutics*, vol. 40, no. 1, pp. 21–30, 2017.

[6] A. Borboni, K.V.V. Reddy, I. Elamvazuthi, M.S. AL-Quraishi, E. Natarajan and S.S Azhar Ali, "The Expanding Role of Artificial Intelligence in Collaborative Robots for Industrial Applications: A Systematic Review of Recent Works", *Machines*, vol. 11, no. 1, art. no. 111, 2023.
[7] S. Robla-Gómez, V.M. Becerra, J.R. Llata, E. González-Sarabia, C. Torre-Ferrero and J. Pérez-Oria, "Working Together: A Review on Safe Human-Robot Collaboration in Industrial Environments", *IEEE Access*, vol. 5, pp. 26754–26773, 2017.
[8] A. De Luca, A. Albu-Schaffer, S. Haddadin and G. Hirzinger, "Collision Detection and Safe Reaction with the DLR-III Lightweight Manipulator Arm", *IEEE/RSJ International Conference on Intelligent Robots and Systems*, pp. 1623–1630, 2006.
[9] M.W. Strohmayr, H. Wörn and G. Hirzinger, "The DLR artificial skin step I: Uniting sensitivity and collision tolerance." *IEEE International Conference on Robotics and Automation,* pp. 1012–1018, 2013.
[10] S. Haddadin, A. De Luca and A. Albu-Schäffer, "Robot Collisions: A Survey on Detection, Isolation, and Identification", IEEE Transactions on Robotics, vol. 33, no. 6, pp. 1292–1312, 2017.
[11] S. Morinaga and K. Kosuge, "Collision detection system for manipulator based on adaptive impedance control law", 2003 IEEE International Conference on Robotics and Automation, vol. 1., Taipei, Taiwan, 2003, pp. 1080–1085.
[12] A. De Luca and R. Mattone, "Sensorless Robot Collision Detection and Hybrid Force/Motion Control", Proceedings of the 2005 IEEE International Conference on Robotics and Automation, Barcelona, Spain, 2005, pp. 999–1004.
[13] M. Iskandar, O. Eiberger, A. Albu-Schaffer, A. De Luca and A. Dietrich, "Collision Detection, Identification, and Localization on the DLR SARA Robot with Sensing Redundancy", IEEE International Conference on Robotics and Automation, Xi'an, China, 2021, pp. 3111–3117.
[14] L. Manuelli and R. Tedrake, "Localizing external contact using proprioceptive sensors: The Contact Particle Filter", IEEE/RSJ International Conference on Intelligent Robots and Systems, Daejeon, South Korea, 2016, pp. 5062–5069.
[15] D. Zurlo, T. Heitmann, M. Morlock and A. De Luca, "Collision Detection and Contact Point Estimation Using Virtual Joint Torque Sensing Applied to a Cobot", IEEE International Conference on Robotics and Automation, London, UK, 2023, pp. 7533–7539.
[16] G. Legnani and I. Fassi, "Robotica industriale - Sezione 2.8: Analisi dinamica diretta e inversa", in Robotica Industriale. Milano: Città Studi Edizioni, 2016, pp. 51–55.
[17] G. Buondonno and A. De Luca, "Combining real and virtual sensors for measuring interaction forces and moments acting on a robot", IEEE/RSJ International Conference on Intelligent Robots and Systems, Daejeon, South Korea, 2016, pp. 794–800.